Comparison of Atmospheric Gradients Estimated From Ground-Based GNSS Observations and Microwave Radiometry

COMPARISON OF ATMOSPHERIC GRADIENTS ESTIMATED FROM GROUND-BASED GNSS OBSERVATIONS AND MICROWAVE RADIOMETRY

Gunnar Elgered[1], **Peter Forkman**[1], **and Tong Ning**[2]

[1]*Chalmers University of Technology, Onsala Space Observatory, SE-439 92 Onsala, Sweden*
[2]*Lantmäteriet (Swedish Mapping, Cadastral and Land Registration Authority), SE-801 82 Gävle, Sweden*

ABSTRACT

Observations over four years from two nearby ground-based Global Navigation Satellite System (GNSS) stations and one microwave radiometer have been used to estimate linear horizontal gradients in the atmosphere. We find that gradients estimated by the radiometer have larger amplitudes than those estimated using data from the Global Positioning System (GPS). One reason for this is that they are estimated, every 15 min, independently of previous estimates, whereas the gradients from GPS are estimated every 5 min using constraints on their variability. We also find that the elevation cutoff angle has a significant impact on the estimated GPS gradients. Decreasing the cutoff angle results in smaller gradient amplitudes. The estimated gradients are not homogeneously distributed in all directions. When studying the largest gradients they all occur during the warmer period of the year, beginning in April and ending in October. Specifically, for the 25 events with the largest gradient amplitudes from the GPS data, we find that the vast majority of them are associated with the passage of weather fronts.

Key words: GNSS; microwave radiometry; water vapour; horizontal gradients.

1. INTRODUCTION

It is common practice to estimate horizontal linear gradients in space geodetic data processing since it has a positive impact on the reproducibility of estimated geodetic parameters using Very Long Baseline Interferoemtry (VLBI) data [1] and Global Positioning System (GPS) data [2].

The use of estimated gradients in meteorology has also been studied, e.g on Corsica in the Mediterranean Sea [3], during the hurricane Harvey in the state of Texas, USA in August 2017 [4], and for Potsdam, Germany [5].

We have estimated linear horizontal gradients in the atmosphere, in the east and in the north directions, using four years of data from two ground-based GPS stations and a water vapour radiometer (WVR) at the Onsala site on the Swedish west coast [6]. The GPS data are from the two collocated stations ONSA and ONS1. Both stations are included in the IGS, EUREF, and SWEPOS networks.

Figure 1: The GNSS installations ONSA (top, left) and ONS1 (top, right) and the WVR Konrad (bottom).

The GPS gradients are estimated for both the ONSA and the ONS1 stations, using three different elevation cutoff angles: 3°, 10°, and 20°, with a temporal resolution of 5 min. The WVR observations are acquired at elevation angles $> 20°$ in order to avoid emission from the ground. Approximately 100 observations spread over the sky during 15 min are used to estimate the east and the north wet gradients. The GPS antenna installations and the WVR are shown in Fig. 1. In this study we focus on the wet gradients. The hydrostatic gradients from the European Centre for Medium-Range Weather Forecasts (ECMWF) [7] are subtracted from the total gradients, originally estimated from the GPS data. For a detailed description of the data processing done in order to estimate the GPS and the WVR gradients, see [6].

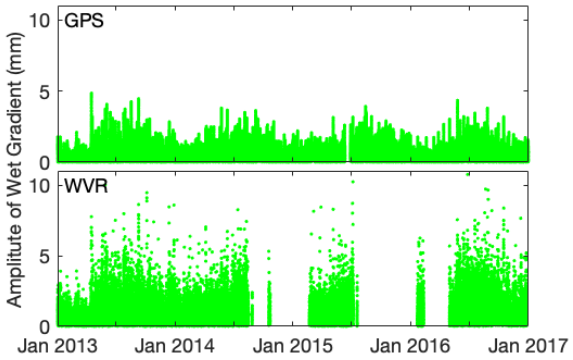

Figure 2: Time series of GPS and WVR wet gradient amplitudes. The GPS gradients are from the ONSA station and a 3° elevation cutoff angle. The distributions of these amplitudes are shown in Fig. 3, and in Fig. 4 we show them as a function of their direction (azimuth angle).

2. CHARACTERIZATION OF GRADIENTS

The entire data set spans four years, 2013–2016. North and east components of the horizontal gradients are estimated and thereafter also combined to a time series of gradient amplitudes. These are shown for the GPS solution using observations acquired with the ONSA station and an elevation cutoff angle of 3° and for the WVR in Fig. 2. The gradients from the WVR are significantly larger compared to the GPS gradients. The WVR gradients are estimated independently of previous values, whereas the GPS gradients are estimated using a constraint for the temporal variability. There is a clear seasonal dependence with larger gradient amplitudes during the warmer and wetter part of the year.

The amplitude distributions are presented as histograms in Fig. 3. The mean amplitude for the whole data set is 0.51 mm for the ONSA station using the 3° elevation cutoff angle (left graph) and increases to 0.75 mm for the solution using the 20° cutoff angle. The mean amplitude for the WVR data (right graph) is 0.87 mm [6].

Fig. 4 depicts all the estimated gradients in terms of their amplitudes and directions. The majority of all gradients are small and of comparable size to their formal uncertainties. Therefore, we now focus on the gradients with the largest amplitudes.

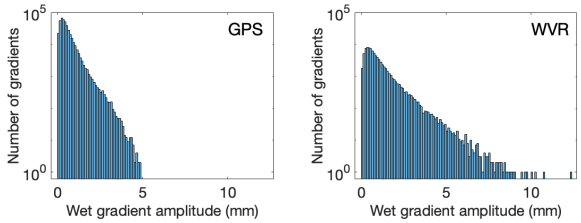

Figure 3: Histograms of the amplitudes of wet gradients from the GPS and the WVR shown in Fig. 2. Note the logarithmic scales on the y-axes.

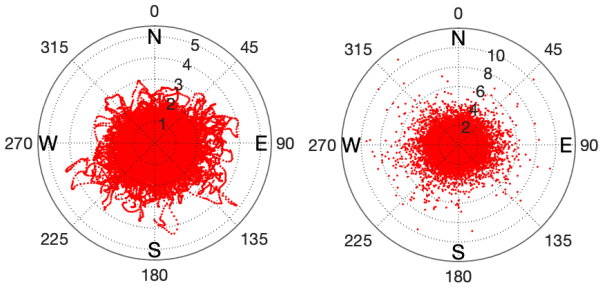

Figure 4: Gradient amplitudes as a function of the azimuth angle for the 408,090 gradients, estimated every 5 min, from the ONSA station using a 3° cutoff angle (left) and the 81,625 gradients, estimated every 15 min, from the WVR (right). Note the different radial scales — their unit is mm.

3. LARGE GRADIENTS

Large wet gradient amplitudes are not evenly distributed with the azimuth angle. This is illustrated in Fig. 5. The GPS stations ONSA and ONS1 give, as expected, similar distributions, but only for the elevation cutoff angles of 3° and 10°. For the 20° cutoff angle the large gradients sensed by ONSA are mainly towards the south-west, whereas ONS1 gradients are mainly in the east direction. We interpret this contradiction to be due to systematic errors appearing when the geometry of the observed satellites becomes weak. This calls for further studies. Although based on the same input data, this is consistent with the earlier result [6] that the GPS gradients from the 3° cutoff angle solution show the highest correlation with the WVR gradients.

Gradients towards the south-west may be due to warm fronts from this direction and gradients towards the east may correspond to cold fronts from the west. Although this is speculative, it makes sense given that the prevailing winds are from the west and that colder air typically come from higher latitudes, i.e. warm fronts arrive from a more southern direction compared to the cold fronts.

In order to examine the cause of large wet gradients in more detail we identified the approximately 25 events with the largest gradient amplitudes (>2 mm) estimated using the results from the GPS station ONSA with an elevation cutoff angle of 3° (upper graph in Fig. 2). They all occurred during the period of the year beginning in April and ending in October. We expanded the time scale and studied the north and the east gradients together with the equivalent zenith wet delay (ZWD) for the six GPS solutions, and the corresponding gradients and ZWD estimated from the WVR data. A rapid change in the ZWD is an indication of the passage of a frontal system and the corresponding shift between drier and more humid air masses. Additional information regarding the location of frontal systems was obtained from the archives of weather analyses, typically available every 6 h, produced by the UK Met Ofiice and the Deutche Wetter Dienst and accessed via http://www1.wetter3.de/.

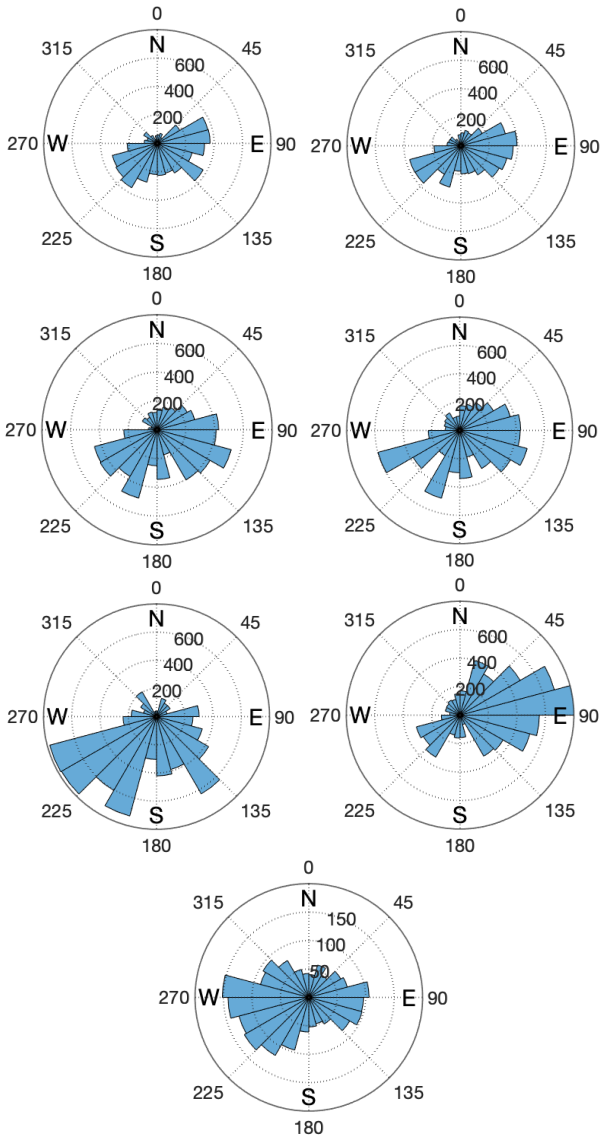

Figure 5: Distribution of the directions of large gradients. The graphs depict the number of gradients in each angular segment of 15°. For the six GPS solutions we set a threshold value for the amplitudes >2 mm. The graphs in the left column are for the ONSA station, applying elevation cutoff angles of 3°, 10°, and 20° (from the top). Similarly the graphs in the right column are for the ONS1 station. Because the WVR gradients (bottom graph) are in general larger, we use a threshold value of >3 mm in order to cover approximately the same weather events. Note that the WVR observations are all acquired at elevation angles above 20°.

An overall result is that the passage of a weather front is the most common reason for the existence of large gradients. We note that this observation is of course only valid for this specific location, where frontal systems pass regularly. However, also in central Europe large gradients have been detected related to the passage of an occlusion front [8]. We show three examples in Figs. 6, 7, and 8. Here we plot the east and the north gradients estimated by

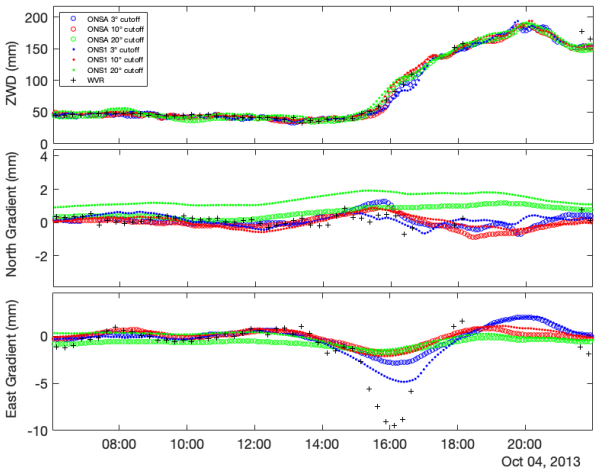

Figure 6: A very distinct warm front passed the site on the 4th of October, 2013. A change in the ZWD from 50 mm to 200 mm in just 4 h is rather unusual, and in fact the west gradient of 10 mm observed by the WVR is one of the largest during the four year period. Comparing the different GPS solutions it is a bit surprising that the east gradients for ONSA and ONS1 differ significantly between the 3° cutoff angle solutions, although they agree better with the WVR gradients compared to the gradients from the solutions using the other cutoff angles. The difference between ONSA and ONS1 may call for additional studies. We note that the north gradients estimated using the 20° cutoff angle seem inaccurate.

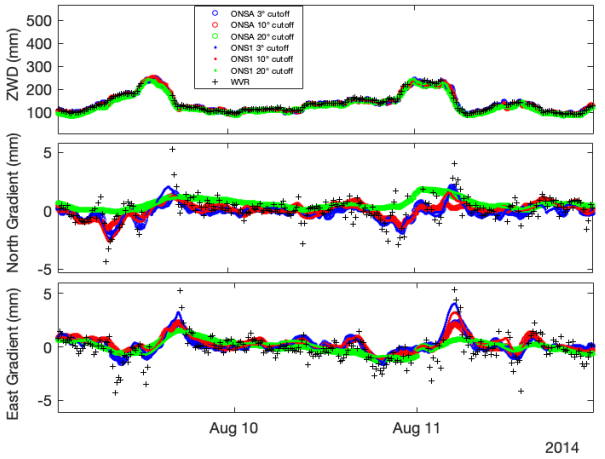

Figure 7: Two cold front passages are shown in this example: in the afternoon of 9th of August and in the morning of 11th of August. There are also significant gradients detected in the GPS solutions, south gradients before the cold front arrives on the 9th of August, using the 3° and 10° cutoff angles, which are supported by the WVR data. Also in this example the gradients estimated by the 20° cutoff angle solution show significant differences compared to the other time series. The figure also depicts that the east gradients from ONS1 are larger than those from ONSA at the front passage around 5 UT of the 11th of August.

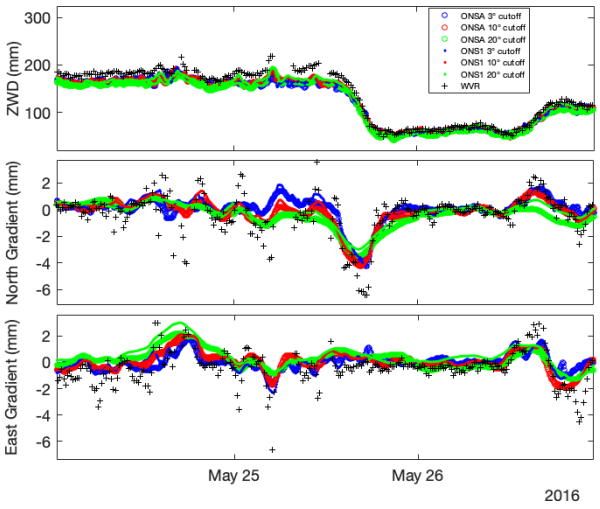

Figure 8: In this example the estimated gradients from all GPS solutions and the WVR all have large values in the south direction around 17 UT on 25th of May 2016. Before the cold front arrives at the station we also see variability in the estimated gradients, and especially in the WVR time series. Although the WVR gradients correlate with the GPS gradients we cannot rule out that rain or large liquid drops have had a negative impact on the accuracy of the WVR gradients. This may be in combination with small scale structures in the atmosphere implying that the GPS and the WVR observations sample different atmospheric paths that are not well described by the linear model.

both ONSA and ONS1 data for each one of the three different elevation cutoff angles and the gradients estimated from the WVR data. Note that precipitation is often associated with frontal system and that this is the reason why WVR data are missing during some periods. The algorithm which corrects the sky brightness temperatures for liquid water drops does not hold during rain. Therefore, all WVR observations resulting in an equivalent zenith liquid water content <0.7 mm have been ignored.

4. CONCLUSIONS AND FUTURE WORK

We find that the estimated horizontal gradients are not homogeneously distributed in all directions. For the Onsala site there is a preference for east-west gradients, possibly caused by that the prevailing winds are from the west and that it is a coastal station, with the coast line oriented in the north-south direction.

Related to these observations we conclude that for the weather conditions at this site the passage of frontal systems is the cause for the largest gradients in the atmosphere. A consequence is that they are not long lived, typically just a few hours or less.

The elevation cutoff angle has a significant impact on the estimated gradients. We interpret that this is a combined effect of a weaker geometry for higher cutoff angles and systematic effects in the electromagnetic environment of the antenna. We do not recommend elevation cutoff angles as high as 20° when there is a goal to estimate accurate horizontal gradients. This conclusion may change if multi-GNSS is used, providing more satellites meaning more observations and a better geometry [9]. We recommend further studies related to these issues.

REFERENCES

[1] Chen, G., & Herring, T. A.: Effects of atmospheric azimuthal asymmetry on the analysis of space geodetic data, *J. Geophys. Res.*, 102(B9), 20489–20502, https://doi.org/10.1029/97JB01739, 1997.

[2] Bar-Sever, Y.-E., Kroger, P. M., & Börjesson, J. A. (1998). Estimating horizontal gradients of tropospheric path delay with a single GPS receiver, *J. Geophys. Res.*, 103, 5019–5035, https://doi.org/10.1029/97jb03534.

[3] Morel, L., Pottiaux, E., Durand, F., Fund, F., Boniface, K., de Oliveira, P. S., & Van Baelen, J. (2015). Validity and behaviour of tropospheric gradients estimated by GPS in Corsica, *Adv. Space Res.*, 55, 135–149, https://doi.org/10.1016/j.asr.2014.10.004.

[4] Graffigna, V., Hernández-Pajares, M., Gende, M. A., Azpilicueta, F. J., & Antico, P. L. (2019). Interpretation of the tropospheric gradients estimated with GPS during hurricane Harvey, *Earth and Space Science*, 6, https://doi.org/10.1029/2018EA000527.

[5] Zus, F., Douša, J., Kačmařík, M., Václavovic, P., Dick, G., & Wickert, J. (2019). Estimating the impact of global navigation satellite system horizontal delay gradients in variational data assimilation, *Remote Sensing*, 11, 41, https://doi.org/10.3390/rs11010041.

[6] Elgered, G., Ning, T., Forkman, P., & Haas R. (2019). On the information content in linear horizontal delay gradients estimated from space geodesy observations, *Atmos. Meas. Tech.*, 12, 3805–3823, https://doi.org/10.5194/amt-12-3805-2019.

[7] Boehm, J. & Schuh, H. (2007). Troposphere gradients from the ECMWF in VLBI analysis, *J. Geod.*, 81, 403–408, https://doi.org/10.1007/s00190-007-0144-2.

[8] Kačmařík, M., Douša, J., Zus, F., Václavovic, P., Balidakis, K., Dick, G., & Wickert, J. (2019). Sensitivity of GNSS tropospheric gradients to processing options, *Ann. Geophys.*, 37, 429–446, https://doi.org/10.5194/angeo-37-429-2019.

[9] Li, X., Zus, F., Lu, C., Ning, T., Dick, G., Ge, M., Wickert, J., & Schuh, H. (2015). Retrieving high-resolution tropospheric gradients from multiconstellation GNSS observations, *Geophys. Res. Lett.*, 42(10), 4173–4181, https://doi.org/10.1002/2015GL063856.